Science Translational Medicine
AAAS

www.sciencetranslationalmedicine.org/cgi/content/full/10/422/eaag1782/DC1

Supplementary Materials for

A miRNA181a/NFAT5 axis links impaired T cell tolerance induction with autoimmune type 1 diabetes

Isabelle Serr, Martin G. Scherm, Adam M. Zahm, Jonathan Schug, Victoria K. Flynn, Markus Hippich, Stefanie Kälin, Maike Becker, Peter Achenbach, Alexei Nikolaev, Katharina Gerlach, Nicole Liebsch, Brigitta Loretz, Claus-Michael Lehr, Benedikt Kirchner, Melanie Spornraft, Bettina Haase, James Segars, Christoph Küper, Ralf Palmisano, Ari Waisman, Richard A. Willis, Wan-Uk Kim, Benno Weigmann, Klaus H. Kaestner, Anette-Gabriele Ziegler, Carolin Daniel*

*Corresponding author. Email: carolin.daniel@helmholtz-muenchen.de

Published 3 January 2018, *Sci. Transl. Med.* **10**, eaag1782 (2018)
DOI: 10.1126/scitranslmed.aag1782

The PDF file includes:

Other Supplementary Material for this manuscript includes the following:
(available at www.sciencetranslationalmedicine.org/cgi/content/full/10/422/eaag1782/DC1)

Table S1 (Microsoft Excel format). Primary source data.

Materials and Methods

Human subjects

No islet autoimmunity: First degree relatives of patients with T1D who are islet autoantibody negative (n=11; median age= 8 years, interquartile range (IQR)= 6-12 years, six males, five females); recent onset of islet autoimmunity: subjects with multiple islet autoantibodies for less than 5 years (n=7, median age= 5 years, IQR= 4-14 years, five males, two females); persistent autoimmunity: subjects with multiple islet autoantibodies for more than 5 but less than 10 years (n=9, median age= 14 years, IQR=10-17.5 years, 7 males, two females); longterm autoimmunity: subjects with multiple islet autoantibodies for more than a decade who did not yet develop T1D (n=7, median age= 15 years, IQR= 14-25 years, three males, four females).

Mice

Female NOD/ShiLtJ mice were obtained from the Jackson Laboratory and stratified according to their insulin autoantibody status (insulin autoantibody (IAA) assay as outlined below). NFAT5ko mice were kindly provided by Christoph Küper: These mice carry an *Nfat5* allele with a *loxP*-flanked exon 4 (NFAT5^{flx}) and a *Cre*-ERT2 transgene, encoding a tamoxifen-inducible fusion protein of the Cre recombinase and a mutated estrogen ligand binding domain, under control of the ubiquitinC promoter. As control mice B6.Cg-Tg(UBC-cre/ERT2)1Ejb/J (Jackson Laboratory) were used, which harbor the same *Cre*-ERT2 transgene under control of the ubiquitinC promoter and the *Nfat5* wildtype allele. 10-week-old conditional NFAT5 knockout mice (*Cre*$^{+}$ NFAT5$^{flx/flx}$) or control mice (*Cre*$^{+}$ NFAT5$^{wt/wt}$) were fed a tamoxifen-containing (400 mg/kg) diet (*Cre*-active 400, Lasvendi, Soest, Germany) for 28 days to induce

Cre-mediated deletion of *Nfat5* (*34*). PTEN Tg mice were kindly provided by Manuel Serrano: PTEN Tg mice were created by microinjection of the *B*acterial *A*rtificial *C*hromosome (BAC) RP24-372O16 (obtained from CHORI; http://www.chori.org) into the pronuclei of fertilized oocytes derived from intercrosses between (C57BL6 x CBA)F1 mice. Founders were mated with C57BL6 mice and a transgenic line was selected with a single integration site (*35*). AKAP13 (Brx) haploinsufficient mice were kindly provided by James Segars: Targeted disruption of *brx* was performed using standard homologous recombination by insertion of a Neo^r cassette resulting in elimination of the exon encoding amino acid residues 752 to 1044 of Brx. These residues are required for GEF activity and are conserved throughout Rho GEF family members (*33*). NOD.Cg-*Prkdc*^{scid} *H2-Ab1*^{tm1Gru} *Il2rg*^{tm1Wjl} Tg(HLA-DQA1,HLA-DQB1)1Dv//Sz (NSG HLA-DQ8) mice lack mouse MHC class II and transgenically express human *HLA-DQ8*. These mice were developed by Leonard Shultz at the Jackson Laboratory. These mice are immunodeficient and, after reconstitution with human hematopoietic cells, develop a human immune system (*12*). Donors for reconstitution were sex-matched.

Murine insulin autoantibody (IAA) assay.

Analyses of murine IAAs was done as described previously (*43*) using a mouse high specificity/sensitivity competitive IAA assay in an ELISA format. In brief, high binding 96-well plates (Costar) were coated with human (recombinant) insulin (10 µg/ml, Sigma Aldrich) overnight at 4^{o}C. Nonpecific-blocking was performed with PBS containing 2% BSA for 2 hours at room temperature. Preincubated NOD sera (diluted 1:10) with or without insulin competition were added and incubated for 2 h at room temperature. After 4 wash steps, biotinylated anti–mouse IgG1 (Abcam), diluted 1:10,000 in PBS/BSA was added for 30 min at room temperature. After washing the plate, horseradish peroxidase–labeled streptavidin (BD Biosciences) was

added for 15 min at 1:1000. After 5 additional washing steps TMB substrate solution was added (OptEIA reagent set; BD). Each sample was run in duplicate with and without competition using human insulin.

In a second approach, to determine levels of IAA in NOD mice, a Protein A/G radiobinding assay based on ^{125}I-labelled recombinant human insulin, was applied as previously described (*42*). Serum from non-autoimmune prone Balb/c mice was used as negative control.

Cell staining, flow cytometry and cell sorting.

For murine FACS staining the following monoclonal antibodies were used: From BD Biosciences: anti-CD4 Biotin (GK1.5); from Biolegend: anti-CD25 PerCP-Cy5.5 (PC61), anti-CD44 PE (IM7), anti-Ki67 APC (16A8); from eBioscience: anit-CD4 AlexaFluor700 (RM4-5), anti-CD62L APC (MEL-14), anti-FoxP3 PE (FJK-16s), anti-FoxP3 FITC (FJK-16s).

For PTEN, AKAP13 and NFAT5 staining, unconjugated antibodies from Abcam (PTEN and AKAP13) or from Thermo Scientific (NFAT5) were used: monoclonal: anti-PTEN (Y184), anti-Akap13 (EPR11261), polyclonal: anti-NFAT5 (PA1-023). These antibodies were used in combination with a polyclonal anti-rabbit PE antibody from ebioscience (12-4739-81).

The following monoclonal antibodies were used for human FACS staining: From BD Biosciences: anti-CD25 APC (2A3), anti-CD45RO APC-H7 (UCHL1), anti-CD4 V500 (RPA-T4), anti-HLA-DR PerCP-Cy5.5 (L243); from Biolegend: anti-CD45RA FITC (HI100), anti-CD3 PerCP-Cy5.5 (HIT3a), anti-CD127 PE-Cy7 (A019D5), anti-CD8a Pacific Blue (RPA-T8), anti-CD11b Pacific Blue (ICRF44), anti-CD14 Pacific Blue (HCD14), anti-CD19 Pacific Blue (HIB19), anti-CD3 Alexa Fluor 700 (HIT3a); from eBioscience (San Diego, CA): anti-FOXP3 Alexa Fluor 700 (PCH101), anti-FOXP3 PE (236A/E7).

To detect intracellular protein expression of FOXP3, PTEN, AKAP13 and NFAT5 after surface staining, cells were fixed and permeabilized using the FOXP3 Fix/Perm buffer set (BioLegend). For PTEN, AKAP13 and NFAT5 staining, cells were washed three times after staining with the primary antibody, followed by staining with secondary anti-rabbit PE (1:2000) for 30 minutes. Cells were acquired on the BD FACS AriaIII cell sorting system flow cytometer using FACS Diva software with optimal compensation and gain settings determined for each experiment based on unstained and single-color stained samples. Doublets were excluded based on SSC-A vs. SSC-W plots. Live cell populations were gated on the basis of cell side and forward scatter and the exclusion of cells positive for Sytox Blue (Life Technologies) or Fixable Viability Dye eFluor450 (eBioscience). At least 50,000 gated events were acquired for each sample and analyzed using FlowJo software version 7.6.1 (TreeStar Inc.).

Peptides.

Peptides at >95% purity were synthesized and purified at New England Peptide or at JPT Peptides. Peptide sequences. $HA_{307\text{-}319}$ epitope: HSN-PKYVKQNTLKLAT-OH, natural insulin B:9-23 epitope: H2N-SHLVEALVLVCGERG-OH, four insulin-B-chain-10-23-mimetopes were employed in studies using human $CD4^+$T cells. Peptide selections were made first based on the finding that 22E- and/or 21G- insulin-B:10-23-peptide-variants (ins.mim2=21G-22E; ins.mim.3=21E-22E) were more potent in stimulating murine insulin-specific hybridomas (*10, 45*). Second, two additional insulin-mimetopes with 22E and/or 21G and 14E (ins.mim1= 14E-21G-22E; ins.mim4=14E-21E-22E) were chosen since it had become clear from structural analyses of a human insulin-peptide-HLA-DQ8 complex that glutamic acid (=E) is preferred over arginine at the first MHC-anchor (*46*).

Generation of artificial antigen-presenting cells (aAPCs).

Earlier studies had shown that an indirect coating of fluorescently unlabeled HLA–peptide tetramers on beads via an anti-MHCII antibody provides specific and efficient stimulation of antigen-specific $CD4^+$T cells (*47*). Therefore, we first coated anti-HLA-DQ antibodies (Abcam) to antibody-coupling beads (Dynabeads® Antibody Coupling Kit, Life Technologies) at 20 µg/mg beads followed by coupling with unlabeled HLA-DQ8 tetramers (3 µg per $10x10^6$ beads) to the DQ-antibodies. aAPCs using control tetramers were generated accordingly. For stimulation aAPCs were used at a concentration of 230 µg/ml corresponding to a tetramer concentration of 5 µg/ml.

RT-qPCR primer.

For analysis of miR181a abundance, miRCURY LNA primers for miRNA181a-5p were used. For normalization miRCURY LNA primers for the housekeeper 5s rRNA were used (Exiqon).

For mRNA expression analysis either QuantiTect Primer Assays or designed primers were used: QuantiTect primer assays were used for murine *Pten* and *Akap13* and for human *Ctla4, Pten, Tob1, Nfat5* and *Nfatc2* (Qiagen). Primer sequences for designed primers are:

Sgk1: fwd: CTGCTCGAAGCACCCTTACC rev: TCCTGAGGATGGGACATTTTCA,

Nfat5: fwd: CAGCCAAAAGGGAACTGGAG rev: CAAAGCCTTGCTGTGTTCTG

Foxo1: Fwd: CACCAGGAGAAGCTCCCAAG rev: GGACTGCTCCTCAGTTCCTG.

Levels of *Histone 3* and *18s* were used to normalize target gene expression levels (*Histone*: H3F3A BT020962, primers: fwd: ACT GGC TAC AAA AGC CGC TC, rev: ACT TGC CTC CTG CAA AGC AC; *18s*: QuantiTect Primer assay, Qiagen).

NGS data processing and statistical analysis.

Unwanted adaptor sequences were trimmed from small RNA reads using BTrim (*48*) and quality of sequencing was assessed for trimmed read data with a mean phred quality score of 38, referring to a base call accuracy of 99.99%. Read data was filtered of unwanted RNA fragments by mapping on rRNA, tRNA, snRNA and snoRNA sequences obtained from the Rfam database using bowtie (*49*). Remaining reads were then mapped on mature human miRNA sequences obtained from mirBase (release 20) (*50*) and summed up to read count lists using SAMTools. mRNA read data was processed comparably without unnecessary trimming and filtering. Raw read data was mapped on the human genome (build 37.2) using a gapped alignment for paired end data with bowtie2 (*51*). Finally, read count lists were created by HTSeqcount. Differential expression of miRNA and mRNA was evaluated using DESeq, handling size factor correction and normalisation.

Nanoparticle preparation and characterization.

Materials: Poly(D,L-lactide-co-glycolide) (PLGA) used was Resomer 75:25 (Resomer® RG 752H, Evonik), Chitosan, (Protasan UP CL 113, NovaMatrix) and Polyvinyl alcohol (PVA) (Mowiol 4-88, Kuraray), 5-Fluoresceinamine (FA) Isomer 1 (Sigma-Aldrich, Cas 3326-34-9). The nanoparticles were prepared by an emulsion-diffusion-evaporation method, first described by Kumar et al. (*26*) with slight modifications. The emulsion was prepared using a Harvard syringe pump for controlled dropping speed. Particles were passed through a sterile filter after preparation. The fluorescent labeled particles were prepared with a PLGA- fluoresceinamine

(FA) conjugate. Preparation of FA-labeled PLGA was performed according to the method described by Weiss et al. (*52*). Particles were characterized with Dynamic light scattering (Zetasizer Nano ZS, Malvern). Chitosan PLGA nanoparticles and FA-labeled nanoparticles (in brackets) had a mean hydrodynamic diameter of 146.7 ± 0.8 nm (152.8 ± 1.2nm), polydispersity index 0.068 ± 0.009 (0.056 ± 0.007) and a zeta potential of +29.6 ± 0.3 mV (+29.6 ± 0.7mV).

Analysis of miRNA/nanoparticle uptake by confocal imaging of CD4$^+$T cell cytospins.

Chitosan-coated PLGA nanoparticles (~130 nm in size) with or without fluorescent label (FITC) were received from Claus-Michael Lehr at the Department of Drug Delivery, Helmholtz Institute for Pharmaceutical Research Saarland (HIPS), Saarland University, Germany. In order to test the successful uptake and delivery of miRNA to human and murine CD4$^+$T cells naïve CD4$^+$T cells were stimulated with anti-CD3/anti-CD28 for 18 hours in the presence of FA-labelled nanoparticles complexed with miRIDIAN miRNA transfection control (Dy547). Initially, uptake of nanoparticles by T cells was confirmed by FACS with the identification of a clearly distinguishable FA$^+$-population. For analysis of uptake by confocal imaging human naïve CD4$^+$T cells were stimulated as described above for 18 hours in the presence or absence of nanoparticles and labelled miRIDIAN miRNA mimic transfection control (Dy547). After the stimulation CD4$^+$T cells were washed and fixed. Upon generation of cytospins, intracellular localization of nanoparticles and delivered miRNA was assessed by confocal microscopy.

miRNA181a mimic / antagomir sequences.

Hsa-miR-181a-5p mimic (Exiqon): AACAUUCAACGCUGUCGGUGAGU

Control mimic (negative control 4, Exiqon): GATGGCATTCGATCAGTTCTA

Mmu-miR-181a-5p antagomir (Exiqon): CGACAGCGTTGAATGT

Control antagomir (negative control A, Exiqon): TAACACGTCTATACGCCCA

Immunofluorescent staining of CD4^{+}T cells.

Naive CD4^{+}T cells from wildtype Balbc mice were incubated in pre-coated 96-well plates (5 µg/ml anti-CD3 and anti-CD28) for 54 hours. 100,000 cells per well were used and stimulated with a miR181a mimic [2.1 ng/µl] loaded on PLGA nanoparticles. As a control, cells were stimulated with a control mimic. The cells from 20 separate wells were pooled and fixed in 2% Roti Histofix for 10 minutes at room temperature. For intracellular staining of NFAT5, cells were permeabilized with a permeabilization buffer (eBioscience) followed by protein block (DAKO) for 1 hour. After washing the cells were incubated with rabbit-anti-NFAT5 antibody (ThermoScientific) over night at 4°C. Detection of NFAT5 was done with an Alexa 594 goat-anti-rabbit antibody for 1 hour at room temperature. Extracellular staining of CD3 was done after blocking of proteins with hamster-anti-CD3 antibody (Biolegend) over night at 4°C in the dark. Cells were washed and incubated with a biotinylated anti-armenian hamster antibody (eBioscience) for 1 hour at room temperature followed by streptavidin 488 staining. After nuclei staining with DAPI cells were analyzed by confocal microscopy (Leitz).

Immunofluorescence with STED microscopy

CD4^{+}T cells from respective *in vitro* stimulation conditions were fixed with 2% Roti Histofix for 10 min at RT. After permeabilization with TritonX100 for 5 min and protein block for 10 min with 2% BSA, staining of rat anti-mCD4 antibody (BD) and rabbit-anti-mNFAT5 (ThermoScientific) was performed. Goat-anti-rat^{STAR580} and goat-anti-rabbit^{STAR635P} (Abberior) were used as secondary antibodies. Finally, nuclei were counterstained with DAPI. Negative

control slides were incubated with secondary antibodies only. Cells were analyzed by Abberior 3D STED 2-Channel Super Resolution Microscope (Abberior). The dye STAR580 was excited with a 594 nm pulsed laser, STAR635p with a 640 nm pulsed laser and DAPI with a 405 nm CW laser and depletion of STAR580 + STAR635p was done with a 775 nm pulsed STED laser.

Treg suppression assay

Tregs were induced in an insulin-specific manner using $CD4^+$T cells from female NOD mice and subimmunogenic TCR stimulation. On day 3 Tregs were sort-purified as $CD25^{hi}$ and expanded for 5 days with 1 µg/ml anti-CD3/anti-CD28 and 500 U/ml IL2 in the presence of irradiated feeder cells. On day 5 Tregs were sort purified and co-cultured with CFSE-labeled (0.25µM) effector T cells from female NOD mice at different ratios in the presence of 1 µg/ml anti-CD3/anti-CD28. Effector T cells were rested for 16 h in the absence of IL-2 to force them into synchronous resting before entering the assay. CFSE dilution was analyzed on day 4.

DNA bisulfite conversion and methylation analysis.

Because of the limited availability of sample material, FACS-sorted $CD4^+$T cells were subjected to a combined sample lysis and bisulfite conversion using the EpiTect Plus LyseAll Bisulfite Kit (Qiagen) or the EZ DNA Methylation-Direct Kit (Zymo Research) according to the manufacturer's instructions. For bias-controlled quantitative methylation analysis, a combination of MS-HRM and subsequent Pyrosequencing was performed as described earlier (*53, 54*). Utilizing the PyroMark Assay Design Software 2.0 (Qiagen), PCR primers and the according sequencing primers were designed to cover the area of differential methylation in the first FOXP3 intron initially reported by Baron et al. (*53*) Pyrosequencing data are presented as means of all CpG-sites analysed due to high homology between methylation levels of the individual sites.

Primers for methylation analysis

PCR primers:

human forward: 50-AAGTTGAATGGGGGATGTTTTTGGGATATAGATTATG-30 ;human reverse: 50-CTACCACATCCACCAACACCCATATCACC-30 ; annealing-temperature: 62°C; murine forward: 50-TTGGGTTTTGTTGTTATAATTTGAATTTGG-30 ; murine reverse: 50-ACCTACCTAATACTCACCAAACATC-30 ; annealing-temperature: 60°C)

sequencing primers:

human: 50-TAGTTTTAGATTTGTTTAGATTTT-30 ; murine: 50-AATTTGAATTTGGTTAGATTTTT-30

Application of *Akap13* siRNA to murine T cells.

Biozol RNA-siRfficient complexes were created by mixing 20 pmol of an Akap13 siRNA (Silencer Select Pre-Designed siRNA Akap13, Ambion) or a negative control siRNA (Silencer Select Negative control no.1, Ambion) with 5% Dextrose and siRfficient solution (Biozol) and incubated for 10min at room temperature according to the manufacturer's instructions. SiRfficient complexes were added to Treg induction assays and Akap13 knockdown was confirmed by RT-qPCR and Treg induction was analyzed by FACS on day 3.

Supplementary figures

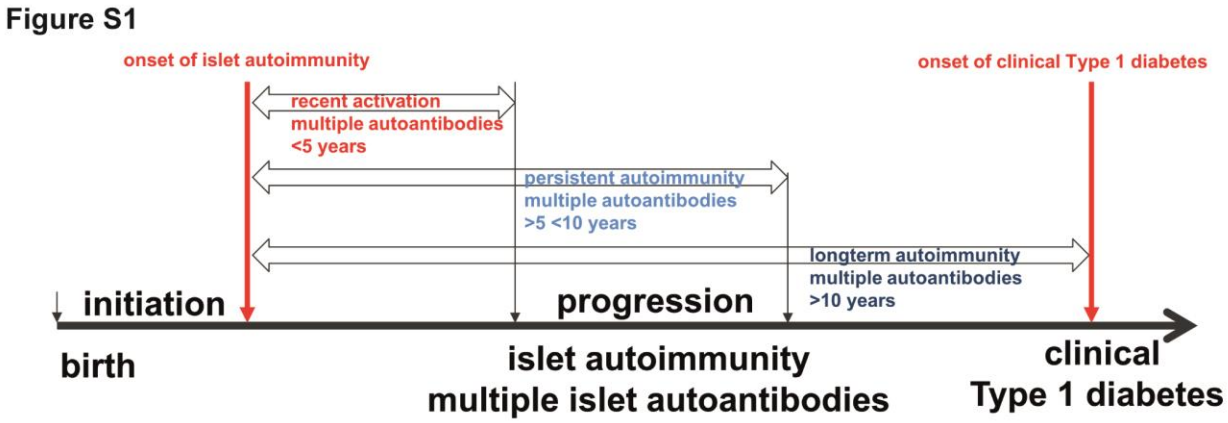

Fig. S1. Categories of human islet autoimmunity in children at risk of developing TD1. Scheme for the progression from islet autoimmunity onset to clinical T1D in children at risk for Type 1 diabetes (T1D). Children at risk for developing T1D were categorized into 4 groups: no islet autoimmunity (islet autoantibody negative), recent activation of islet autoimmunity (islet autoantibodies for less than 5 years), persistent islet autoimmunity (islet autoantibodies for more than 5, but less than 10 years), longterm islet autoimmunity (islet autoantibodies for more than 10 years). The children in all of these categories were pre-T1D without clinical symptoms.

Figure S2

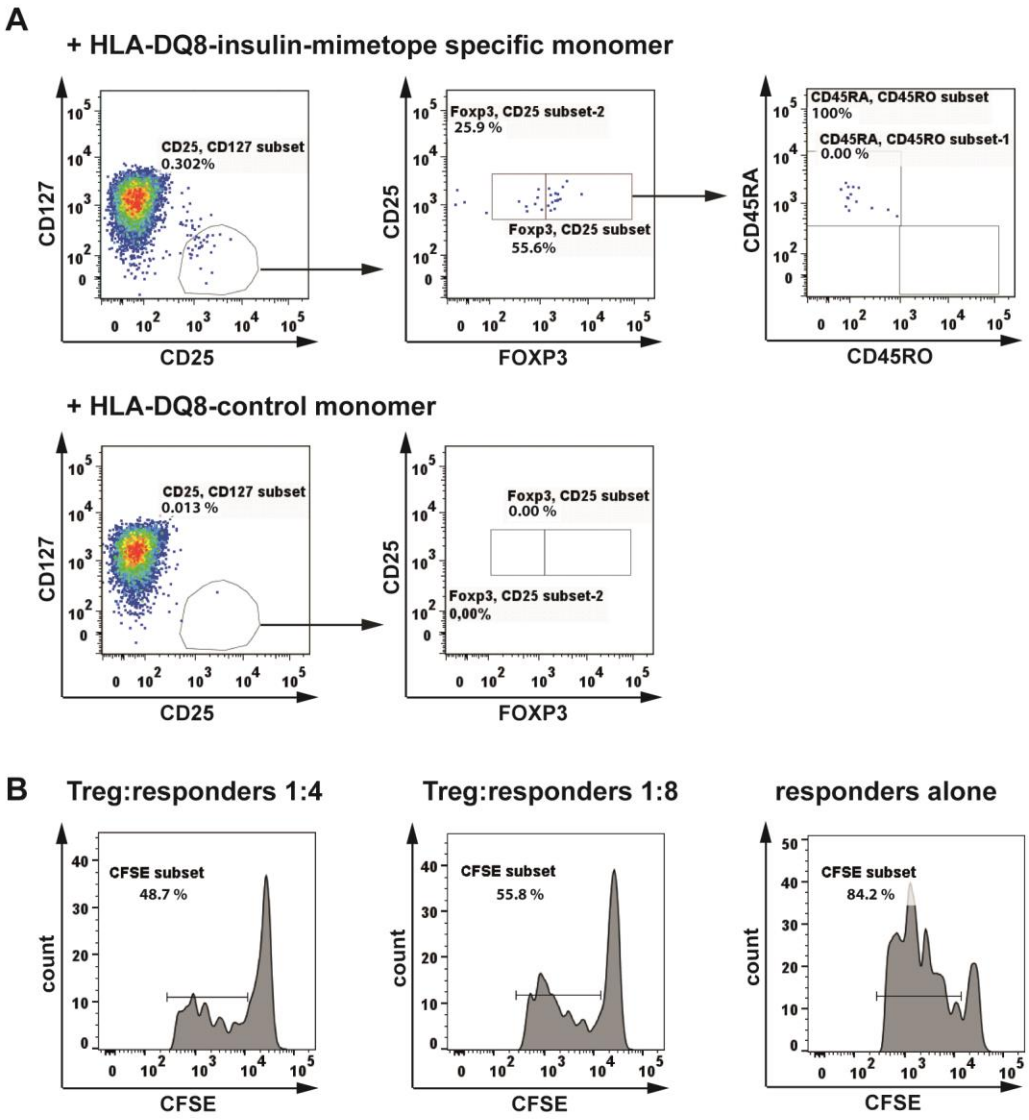

Fig. S2. Identification of insulin-specific T_{regs} after T_{reg} induction assays in vitro. (A) Representative FACS plots for the identification of insulin-specific Tregs induced using subimmunogenic TCR stimulation and HLA-DQ8-insulin-mimetope specific monomers (**upper row**) or HLA-DQ8-control monomers **(lower row)**. Insulin-specific Tregs were first identified as $CD4^{+}CD3^{+}CD127^{lo}CD25^{hi}$ (left plots). Next, within this $CD127^{lo}CD25^{hi}$ population the percentages of $CD25^{hi}FOXP3^{hi}$Tregs were assessed (right plots). **(B)** Representative FACS

histograms for the suppression of effector T cells by *in vitro* induced insulin-specific Tregs indicated by the dilution of the CFSE label. Shown are responders alone as control (right plot), Treg : responder ratio 1:8 (middle plot) and 1:4 (left plot).

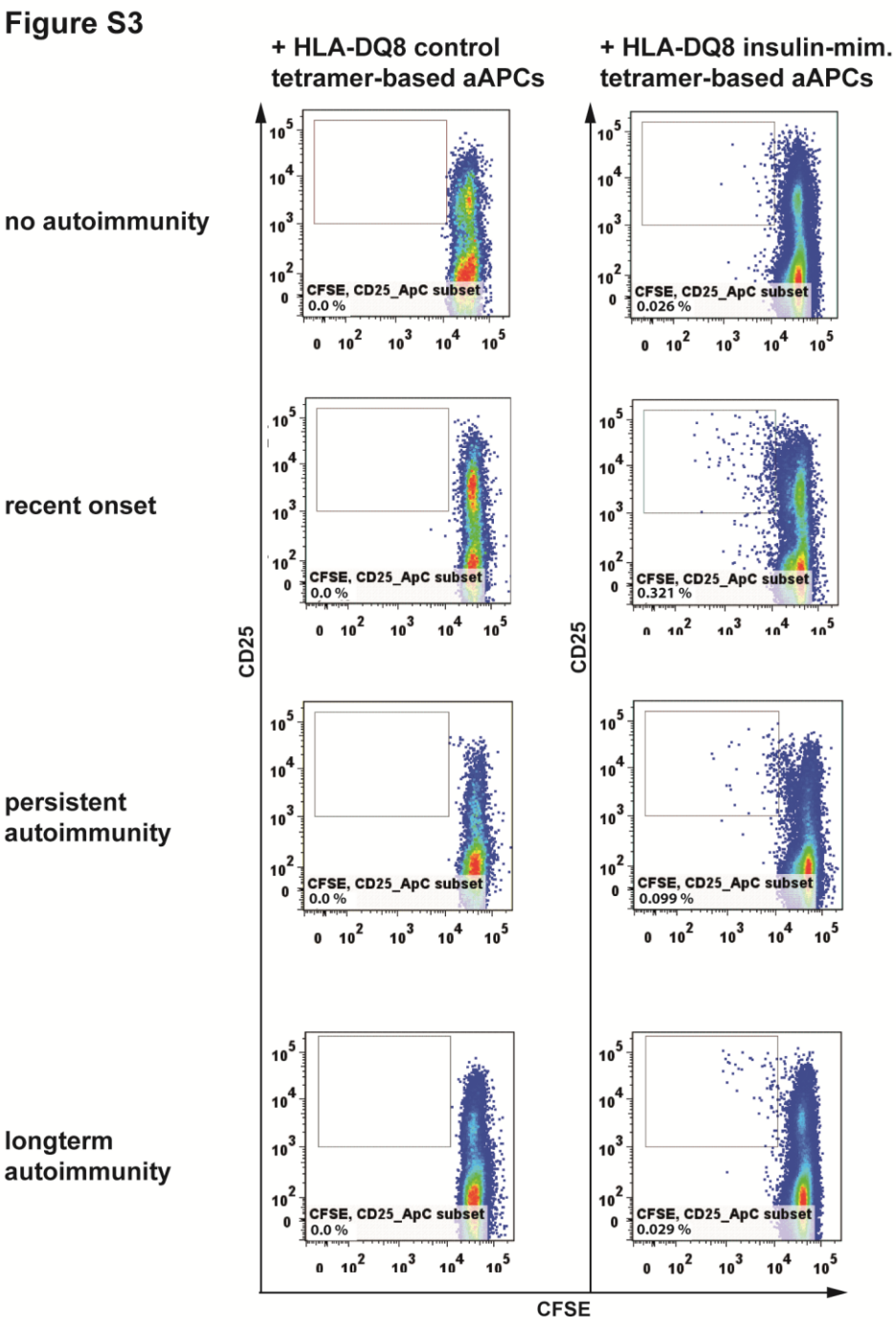

Fig. S3. Insulin-specific CD4$^+$ T cell proliferation in accordance with the duration of islet autoimmunity. Representative FACS plots for the proliferation of CD4$^+$T cells from children with different durations of islet autoimmunity. CD4$^+$T cells were stimulated for 4 days with

either HLA-DQ8 control tetramer-based artificial APCs or HLA-DQ8 insulin-specific tetramer-based artificial APCs. Proliferating $CD4^{+}$T cells were identified as $CFSE^{dim}$ and $CD25^{+}$.

Figure S4

A

name	with islet autoimmunity naive T cells	without islet autoimmunity naive T cells
correction factor	2,418589	1,375624
hsa-let-7g-5p	592646	856529
hsa-miR-21-5p	768185	132532
hsa-miR-150-5p	140610	397796
hsa-miR-26a-5p	159107	302949
hsa-let-7f-5p	149602	159535
hsa-let-7a-5p	124623	114219
hsa-miR-101-3p	50188	103606
hsa-miR-27a-3p	102575	29136
hsa-let-7i-5p	73869	46345
hsa-miR-29a-3p	68294	43906
hsa-miR-92a-3p	23330	59090
hsa-miR-146b-5p	26097	45115
hsa-miR-181a-5p	31836	46518
hsa-miR-26b-5p	42901	21691
hsa-miR-142-3p	31028	18670
hsa-miR-22-3p	41948	3412
hsa-miR-191-5p	23649	20363
hsa-miR-423-3p	17245	25521
hsa-miR-20a-5p	12434	20926
hsa-miR-99a-5p	1560	46931
hsa-miR-361-3p	8073	18985
hsa-miR-423-5p	18205	19654
hsa-miR-142-5p	11399	8104

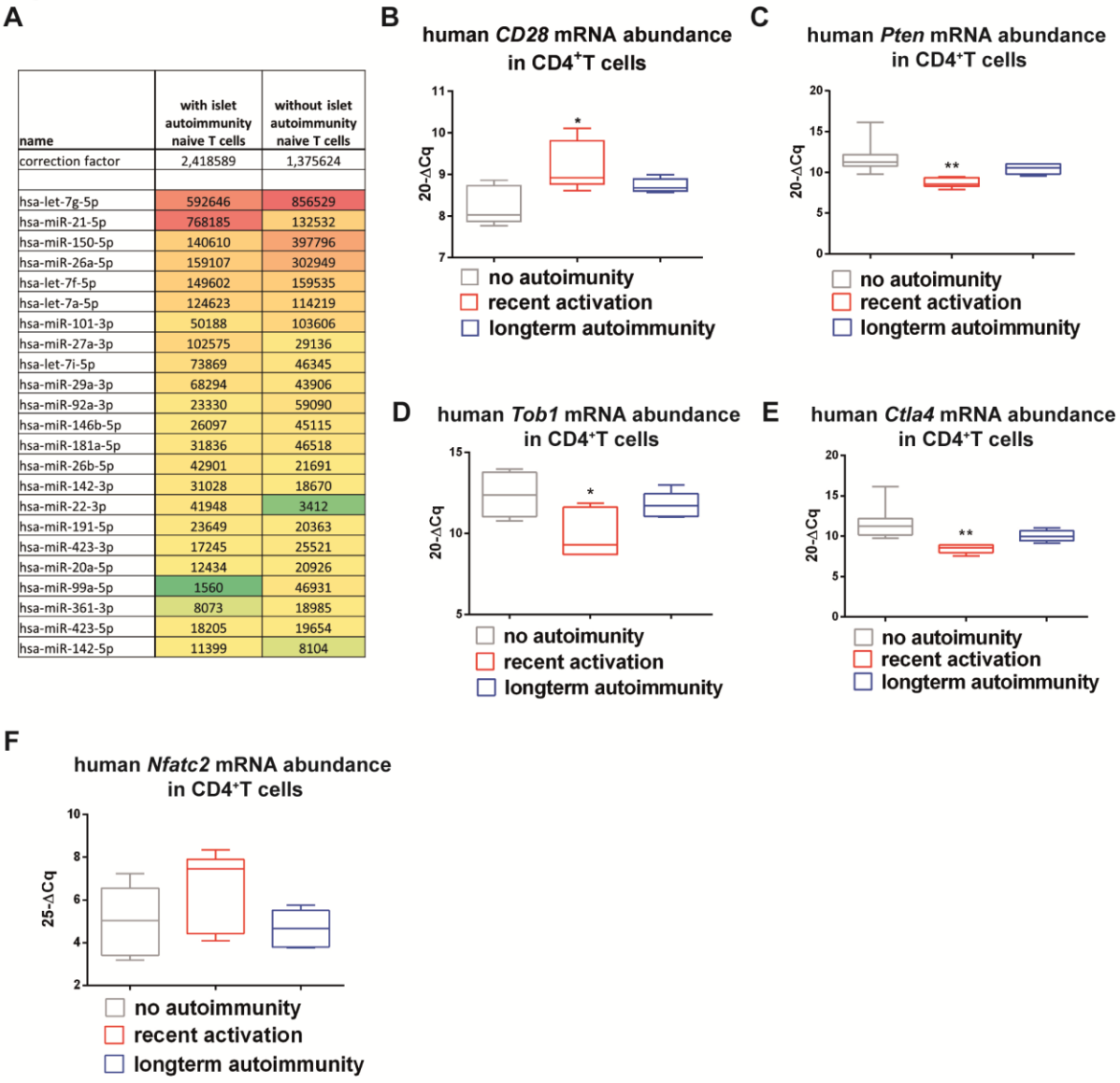

Fig. S4. miR181a-targeted signaling pathways in CD4$^+$ T cells. (A) MiRNA expression profiles in *ex vivo* naïve CD4$^+$T cells from children with or without autoantibodies by NGS of pooled samples (n=4 per group). Shown are a set of most abundant miRNAs. **(B-F)** mRNA abundance of signaling pathways predictively targeted by miRNA181a in *ex vivo* human CD4$^+$T cells as measured by RT-qPCR. *CD28* **(B)** no autoimmunity: n= 6, recent onset of autoimmunity: n= 9, longterm autoimmunity: n= 6. *Pten* **(C)** no autoimmunity: n= 11, recent onset of

autoimmunity: n= 6, longterm autoimmunity: n= 6. *Tob1* **(D)** no autoimmunity: n= 10, recent onset of autoimmunity: n= 6, longterm autoimmunity: n= 10. *Ctla4* **(E)** no autoimmunity: n= 7, recent onset of autoimmunity: n= 6, longterm autoimmunity: n= 6. *Nfatc2* **(F)** no autoimmunity: n= 5, recent onset of autoimmunity: n= 5, longterm autoimmunity: n= 6. **(B-F)** Data are presented as box and whisker plots with min to max values for data distribution. Student's t-test. * $p<0.05$, ** $p<0.01$.

Figure S5

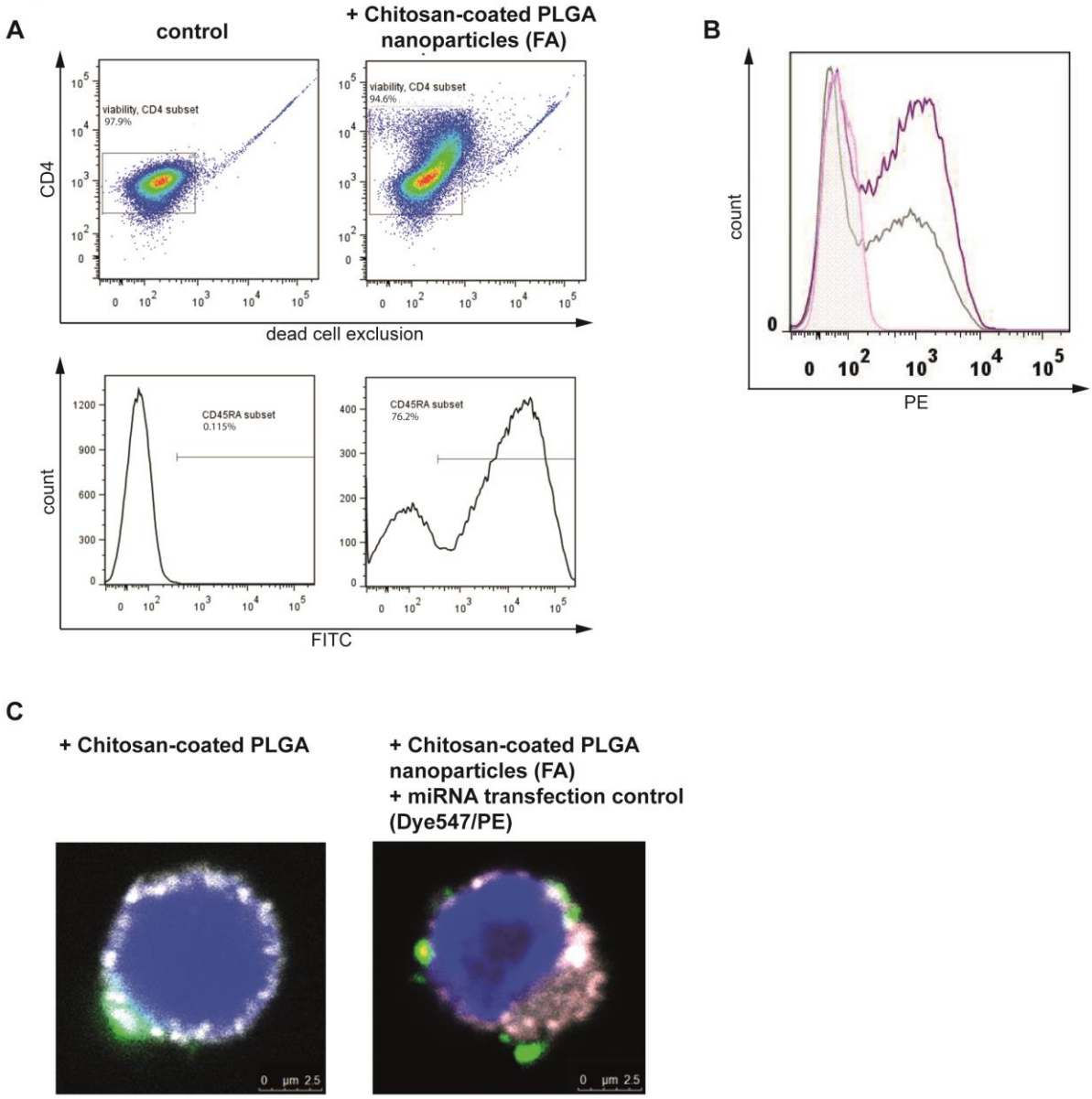

Fig. S5. Nanoparticle-mediated miRNA uptake in CD4$^+$ T cells. (A) Uptake of FA-labeled nanoparticles in Treg induction assays, *in vitro*, as assessed by FACS analyses, first gating on live CD4$^+$T cells (upper row) then on FITC$^+$ T cells (lower row). **(B)** Representative histogram for the FACS analysis of nanoparticle mediated uptake of miRNAs. Naïve CD4$^+$T cells were stimulated with anti-CD3/anti-CD28 for 18 hours in the presence of FA-labeled nanoparticles

(grey line) or Dy457-labeled transfection control miRNA (light pink line) or the combination of both (dark pink line). **(C)** Confocal microscopic images showing the intracellular co-localization of FA-labeled nanoparticles (green) and Dy457-labeled transfected control miRNAs (red) in $CD4^{+}$T cells stimulated with anti-CD3/anti-CD28 for 18 hours.

Figure S6

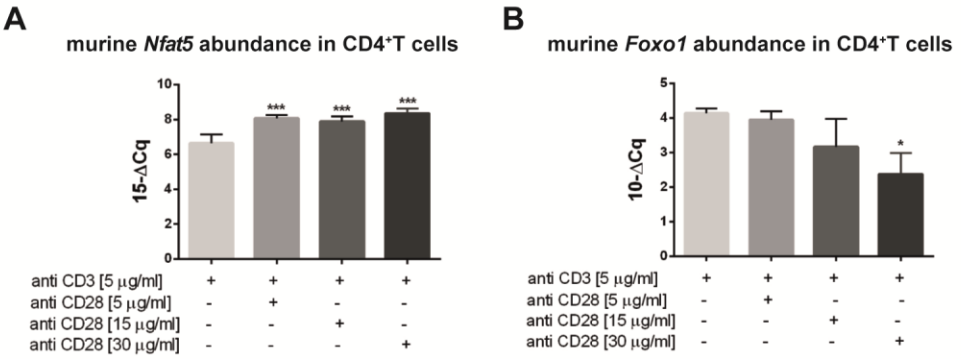

Fig. S6. ***Nfat5*** **and** ***Foxo1*** **expression upon TCR stimulation and increasing doses of costimulation. (A)** Murine mRNA abundance of *Nfat5* in $CD4^+$T cells upon *in vitro* stimulation with anti-CD3 and increasing concentrations of anti-CD28 antibodies for 48 hours (n=6 per group). **(B)** Murine mRNA abundance of *Foxo1* in $CD4^+$T cells from *in vitro* Treg induction assays with anti-CD3 and increasing concentrations of anti-CD28 antibodies (n=3 per group). Data represent the mean ± s.e.m. Student´s t-test. * $p<0.05$, *** $p<0.001$.

Figure S7

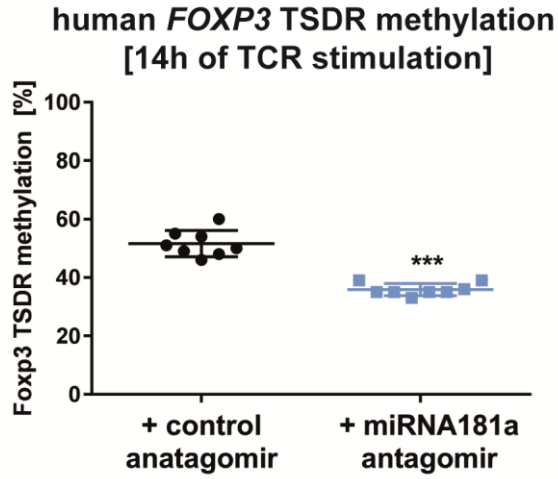

Fig. S7. DNA methylation analysis of the human *FOXP3* TSDR in in vitro–induced T_{regs}. Pyrosequencing analyses of eight successive CpG-sites in the human *FOXP3* TSDR region as methylation in % for human $CD4^{+}CD127^{lo}CD25^{hi}FOXP3^{hi}$Tregs induced with subimmunogenic TCR stimulation of naïve $CD4^{+}$T cells from healthy adults in combination with a control antagomir (left) or a miRNA181a antagomir (right) (n=8 per group), shown is the mean ± s.e.m.. Student´s t-test. ****p*<0.001.

Figure S8

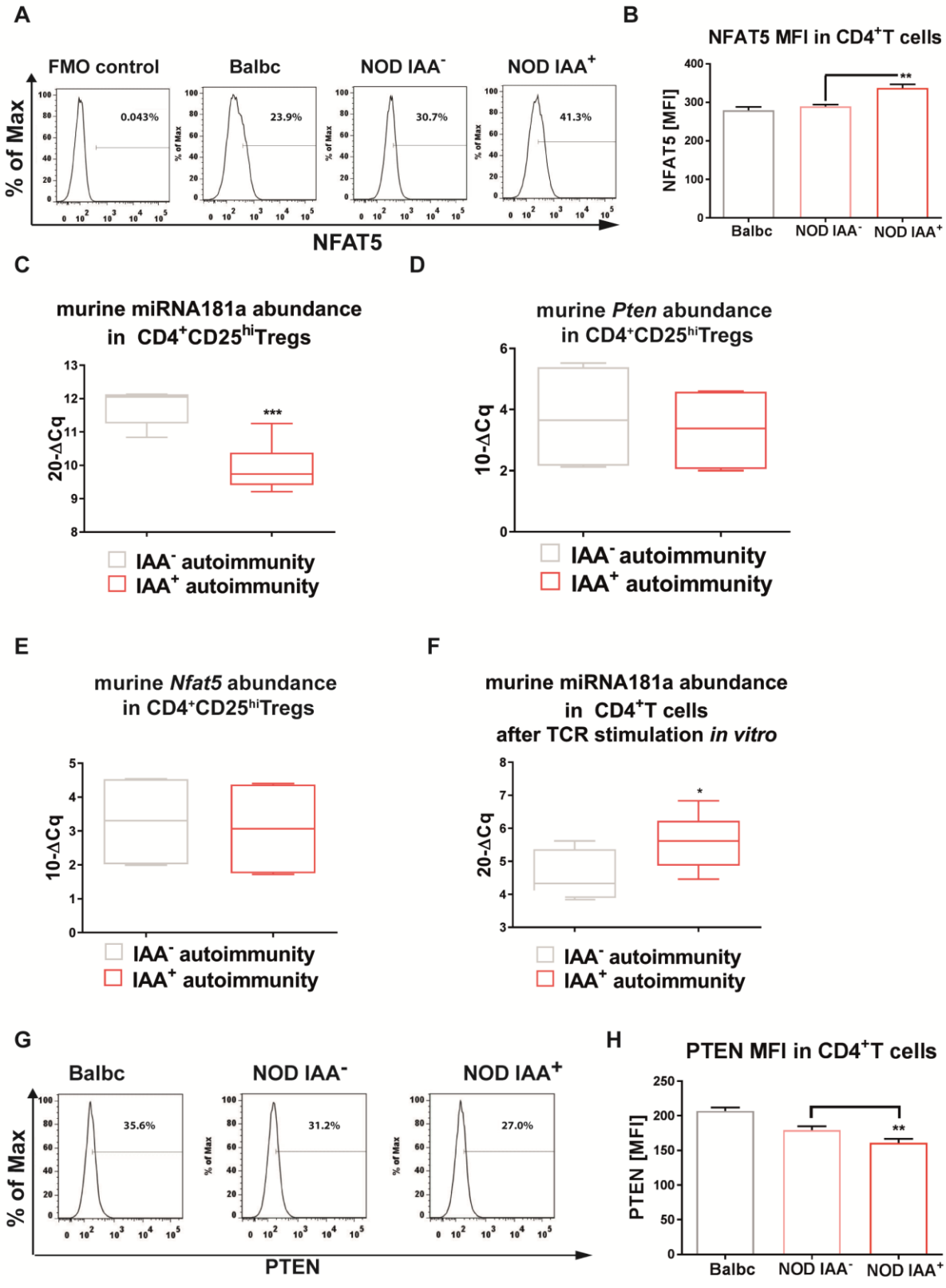
A
FMO control
Balbc
NOD IAA-
NOD IAA+
0.043%
23.9%
30.7%
41.3%
% of Max
NFAT5
B
NFAT5 MFI in CD4+T cells
NFAT5 [MFI]
Balbc
NOD IAA-
NOD IAA+
C
murine miRNA181a abundance
in CD4+CD25hiTregs
20-ΔCq
IAA- autoimmunity
IAA+ autoimmunity
D
murine Pten abundance
in CD4+CD25hiTregs
10-ΔCq
IAA- autoimmunity
IAA+ autoimmunity
E
murine Nfat5 abundance
in CD4+CD25hiTregs
10-ΔCq
IAA- autoimmunity
IAA+ autoimmunity
F
murine miRNA181a abundance
in CD4+T cells
after TCR stimulation in vitro
20-ΔCq
IAA- autoimmunity
IAA+ autoimmunity
G
Balbc
NOD IAA-
NOD IAA+
35.6%
31.2%
27.0%
% of Max
PTEN
H
PTEN MFI in CD4+T cells
PTEN [MFI]
Balbc
NOD IAA-
NOD IAA+

Fig. S8. NFAT5 and PTEN protein expression in CD4$^+$ T cells of NOD mice. (A) Representative histograms for FACS analyses of NFAT5 in *ex vivo* CD4$^+$T cells from Balbc mice and NOD mice with or without IAA$^+$autoimmunity. **(B)** Mean fluorescence intensity (MFI) of NFAT5 staining as in **(A)** (n=4 per group). **(C)** MiRNA181a abundance in *ex vivo* CD4$^+$CD25^{hi}Tregs from NOD mice with (n=9) or without IAA$^+$autoimmunity (n=5). **(D+E)** Murine *Pten* **(D)** and *Nfat5* **(E)** abundance in *ex vivo* CD4$^+$CD25^{hi}Tregs from NOD mice with or without IAA$^+$autoimmunity (n=4 per group). **(F)** MiRNA181a abundance in CD4$^+$T cells from NOD mice with (n=10) or without IAA$^+$autoimmunity (n=4) after *in vitro* TCR stimulation for 48 hours. **(G)** Representative histograms for FACS analyses of PTEN in *ex vivo* CD4$^+$T cells from Balbc mice and NOD mice with or without IAA$^+$autoimmunity. **(H)** MFI of PTEN staining as in **(E)** (n=4 per group). Data are presented as box and whisker plots with min and max values for data distribution **(C-F)** or as the mean ± s.e.m. **(B+H)**. Student´s t-test. * p<0.05, ** p<0.01, *** p<0.001.

Figure S9

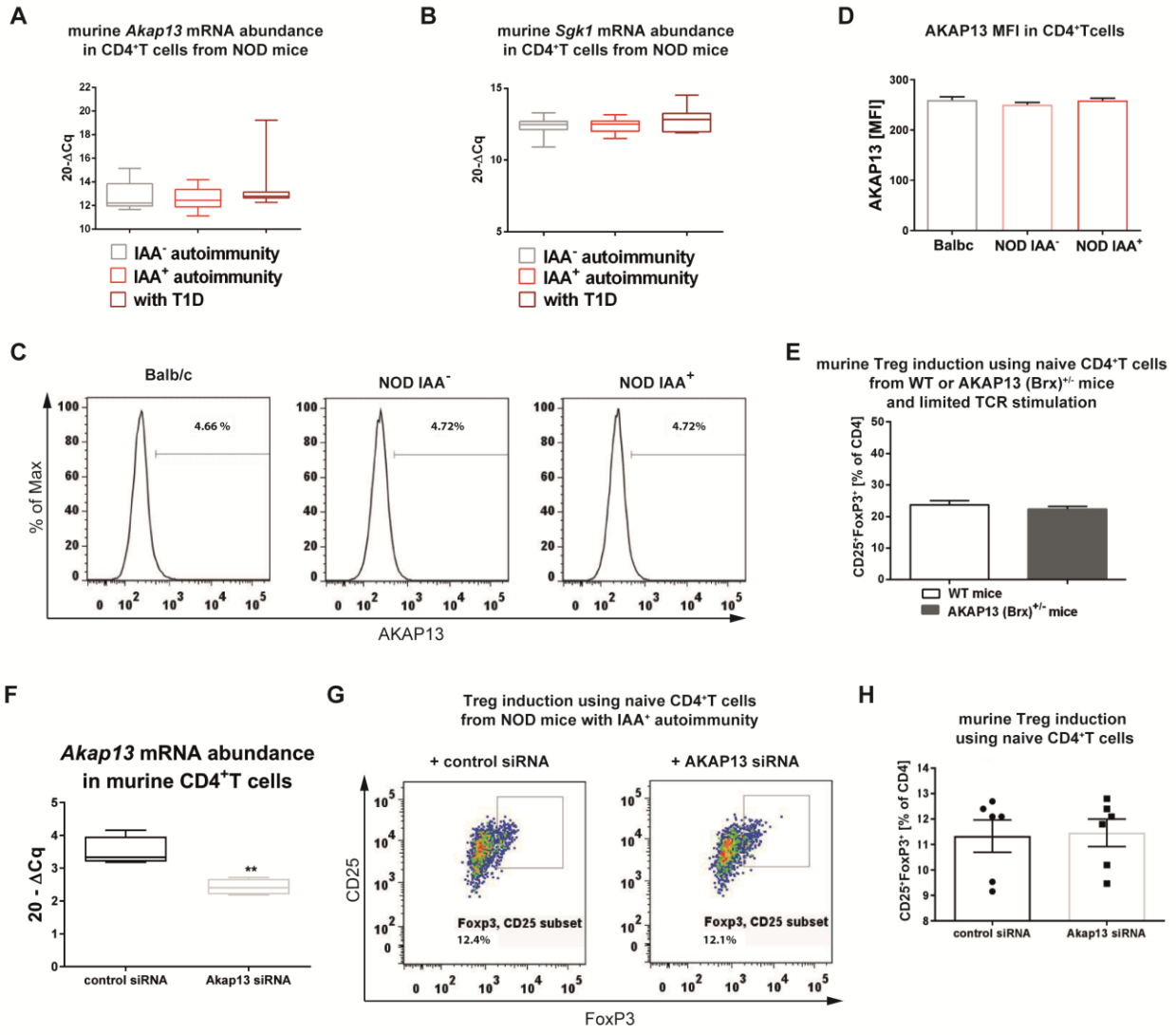

Fig. S9. Hypertonicity-independent NFAT5 induction in CD4$^+$ T cells of IAA$^+$NOD mice. **(A+B)** mRNA expression analysis of *Akap13* **(A)** (n=9 per group) and *Sgk1* **(B)** (IAA$^-$ n=11, IAA$^+$ n=9, with T1D n=8) as measured by RT-qPCR in *ex vivo* CD4$^+$T cells from NOD mice with or without IAA$^+$autoimmunity or with symptomatic T1D. **(C)** Representative histograms for FACS analyses of AKAP13 in *ex vivo* CD4$^+$T cells from Balbc mice and NOD mice with or without IAA$^+$autoimmunity. **(D)** MFI of AKAP13 staining as in **(C)** (n=5 per group). **(E)** Frequencies of CD4$^+$CD25$^+$FoxP3^{hi}Tregs after *in vitro* Treg induction using subimmunogenic

TCR stimulation of naïve $CD4^+$T cells from WT or AKAP13 $(Brx)^{+/-}$ mice (n=4 independent experiments). **(F)** *Akap13* mRNA expression in murine $CD4^+$T cells treated with a control siRNA or an Akap13-specific siRNA for 18 hours (n=4 per group). **(G)** Representative set of FACS plots indicating $CD4^+CD25^+FoxP3^{hi}$Tregs after *in vitro* Treg induction using naïve $CD4^+$T cells from NOD mice with IAA^+autoimmunity and either a control siRNA or an Akap13-specific siRNA. **(H)** Frequencies of $CD4^+CD25^+FoxP3^{hi}$Tregs as in **(G)** (n=6 independent experiments). Data are presented as box and whisker plots with min and max values for data distribution **(A, B, F)** or as the mean ± s.e.m. **(D, E, H)**. Student´s t-test.** $p<0.01$.

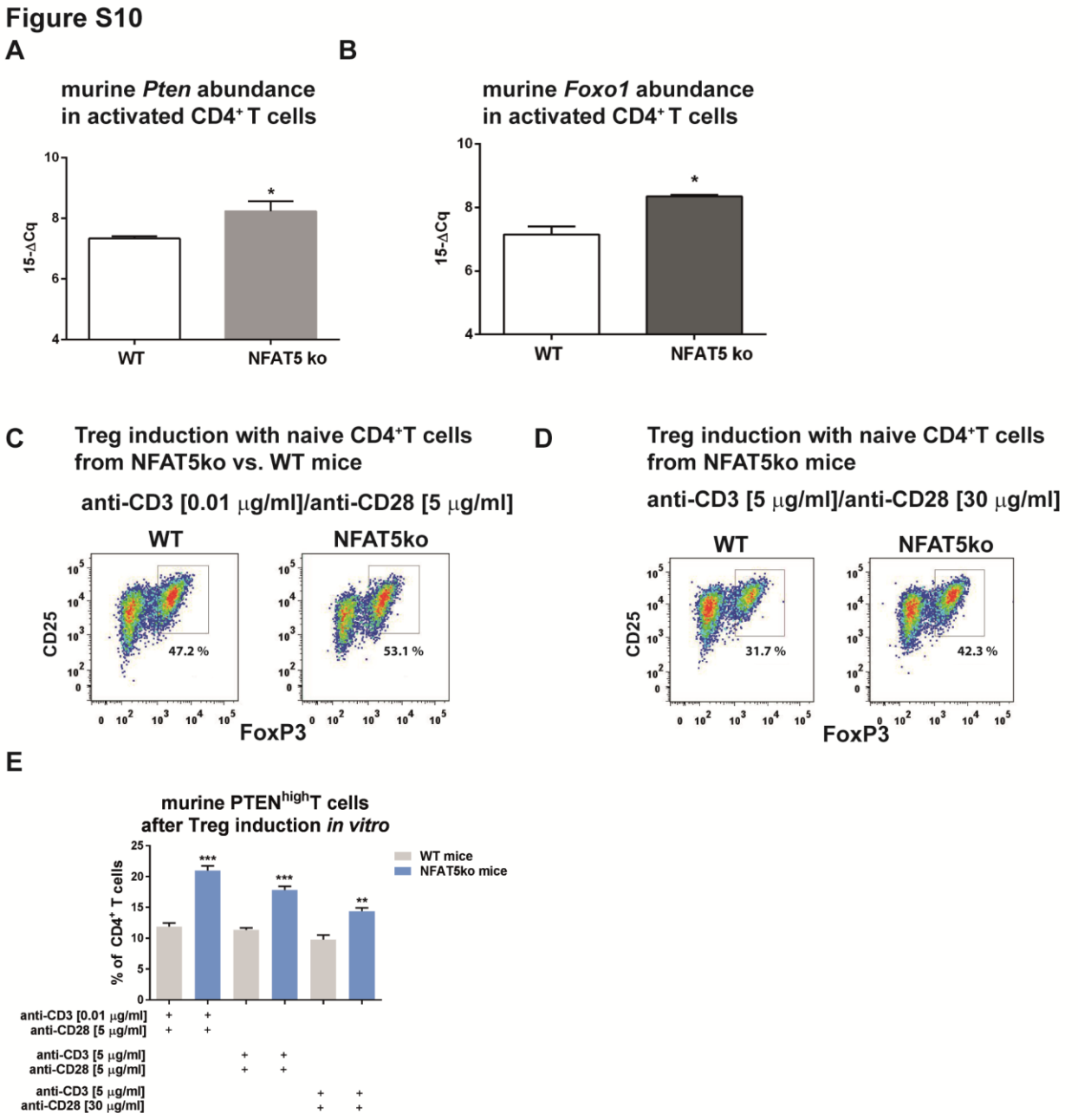

Fig. S10. *Pten* and *Foxo1* expression in CD4⁺ T cells from NFAT5ko mice. (A+B) murine *Pten* **(A)** and *Foxo1* **(B)** mRNA abundance in *ex vivo* activated CD4⁺T cells from WT or NFAT5ko mice (n=3 per group). **(C+D)** Representative set of FACS plots indicating CD4⁺CD25⁺FoxP3^{hi}Tregs after *in vitro* Treg induction using CD4⁺T cells from NFAT5ko mice and stimulation with 0.01µg/ml anti-CD3 and 5µg/ml anti-CD28 **(C)** or 5µg/ml anti-CD3 and

30µg/ml anti-CD28 **(D)**. **(E)** Frequencies of $CD4^{+}PTEN^{hi}$T cells after Treg induction *in vitro* with 5µg/ml anti-CD3 and 5µg/ml anti-CD28 or as in **(C+D)** (n=4 independent experiments). **(A, B, E)** Data represent the mean ± s.e.m.. Student´s t-test. * $p<0.05$, ** $p<0.01$.

Figure S11

A Treg induction with naive CD4⁺T cells from NFAT5ko mice

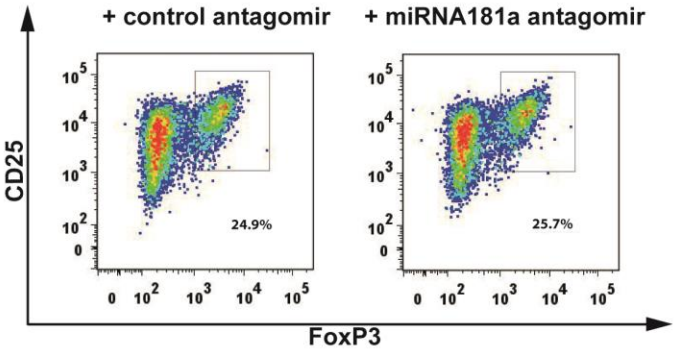

anti-CD3 [5 μg/ml]/anti-CD28 [5 μg/ml]

B Treg induction with naive CD4⁺T cells from NFAT5ko mice

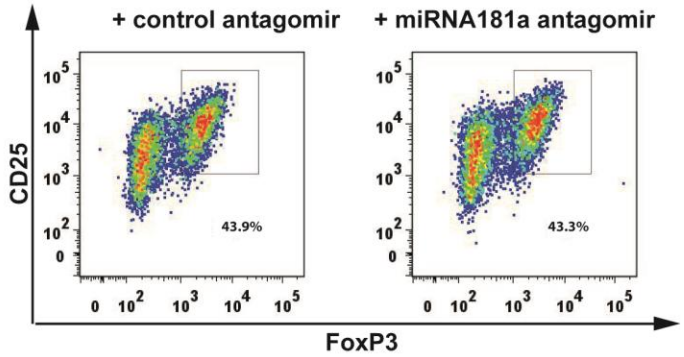

anti-CD3 [0.01 μg/ml]/anti-CD28 [5 μg/ml]

C Treg induction with naive CD4⁺T cells from NFAT5ko mice

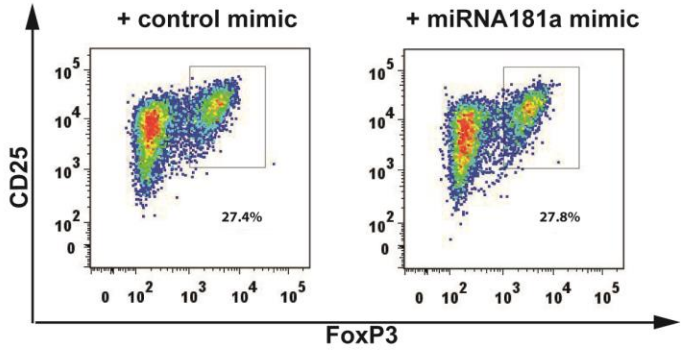

anti CD3 [5 μg/ml]/anti-CD28 [5 μg/ml]

D Treg induction with naive CD4⁺T cells from NFAT5ko mice

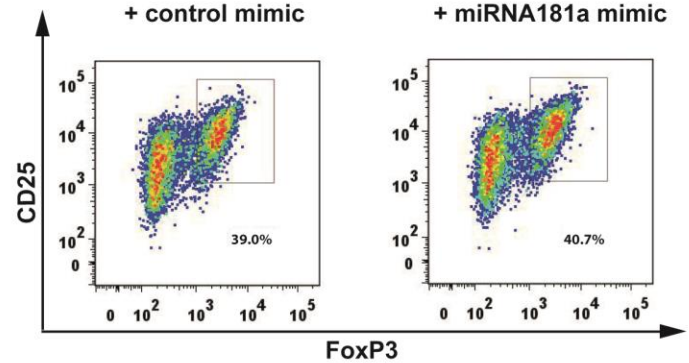

anti-CD3 [0.01 μg/ml]/anti-CD28 [5 μg/ml]

Fig. S11. T_{reg} frequencies after in vitro induction using $CD4^+$ T cells from NFAT5ko animals. (A-D) Representative FACS plots indicating $CD4^+CD25^+FoxP3^{hi}$Tregs induced *in vitro* from $CD4^+$T cells of NFAT5ko animals with addition of a miRNA181a antagomir **(A+B)** or mimic **(C+D)** and different concentrations of anti-CD3 and anti-CD28. 5µg/ml anti-CD3 and 5µg/ml anti-CD28 **(A+C)**, 0.01µg/ml anti-CD3 and 5µg/ml anti-CD28 **(B+D)**.

Figure S12

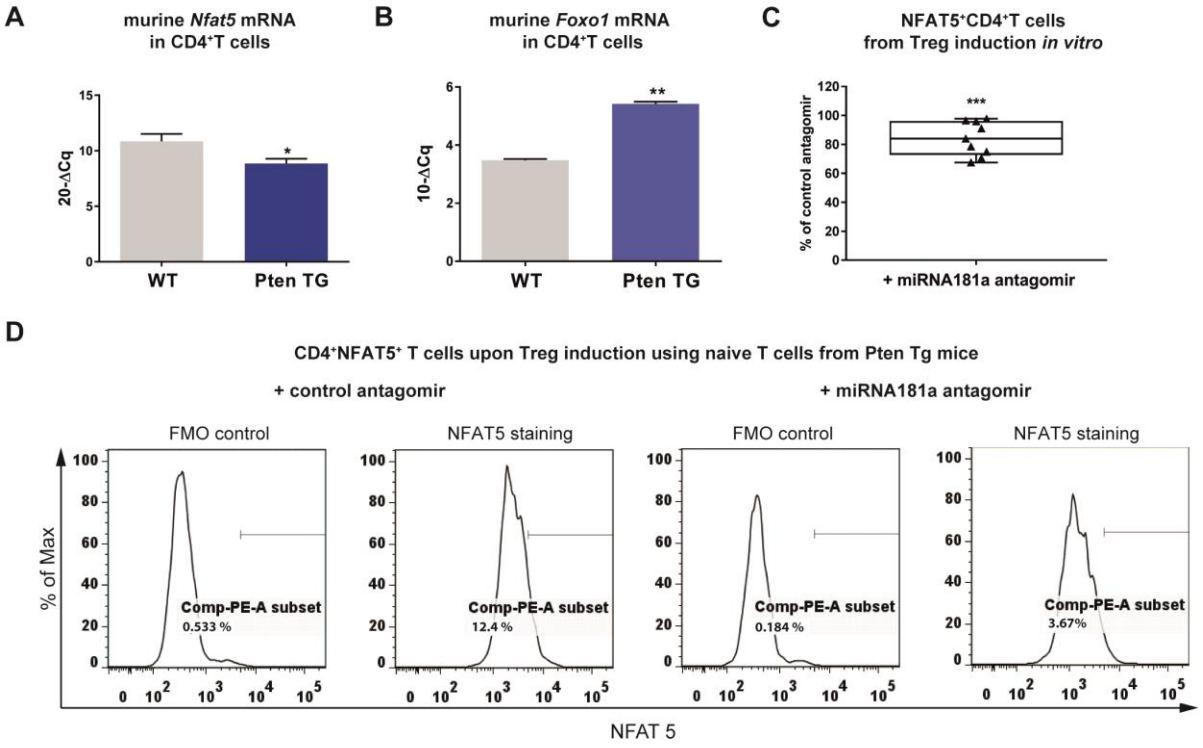

Fig. S12. *Nfat5* and *Foxo1* expression in CD4$^+$ T cells of PTEN Tg mice. (A+B) murine *Nfat5* **(A)** and *Foxo1* **(B)** mRNA abundance in *ex vivo* CD4$^+$T cells with an activated phenotype from WT or PTEN Tg mice (n=4 per group). **(C)** Frequencies of NFAT5+CD4+T cells treated as in **(D)** (n=9 per group), presented as % of control antagomir. **(D)** Representative histograms of FACS stainings for NFAT5 in CD4$^+$T cells from PTEN Tg mice after *in vitro* Treg induction using shortterm TCR stimulation and addition of a control or miRNA181a antagomir. Data are presented as box and whisker plots with min to max values for data distribution **(C)** or as mean ± s.e.m. **(A+B)**. Student´s t-test. * p<0.05; ** p<0.01; ***p<0.001.

Figure S13

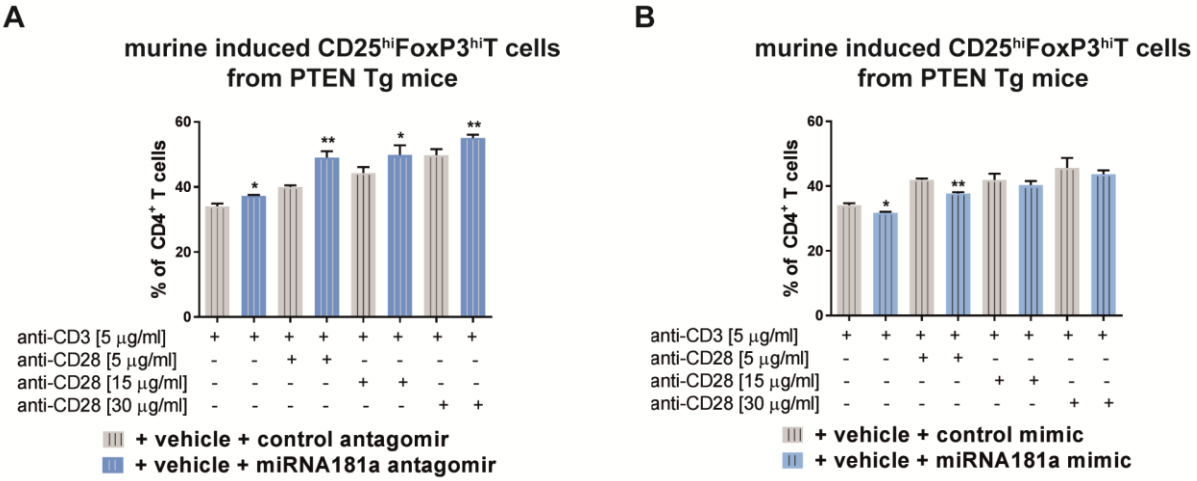

Fig. S13. Effect of an miRNA181a antagomir or mimic on T_{reg} induction from PTEN Tg mice with decreasing anti-CD28 stimulation. (A+B) Frequencies of $CD4^+CD25^+FoxP3^+$Tregs upon Treg induction from PTEN Tg mice in the presence of a miRNA181a or control antagomir **(A)** or mimic **(B)** upon stimulation with anti-CD3 and increasing concentrations of anti-CD28 (n=4 independent experiments). Data are presented as mean ± s.e.m.. Student´s t-test. *p<0.05, **p<0.01

Figure S14

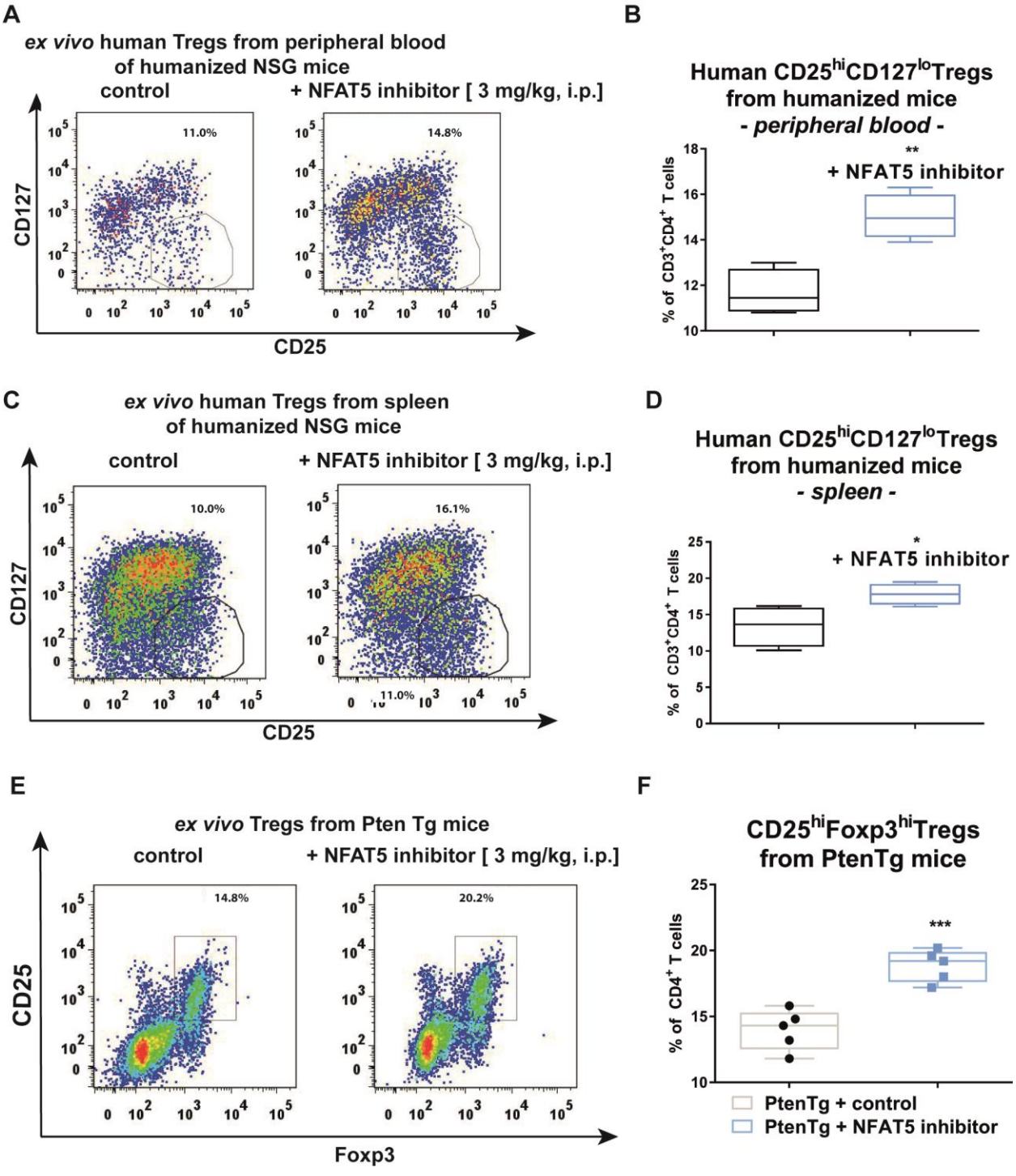

Fig. S14. Effect of NFAT5 inhibition in CD4$^+$ T cells from humanized NSG mice or from PTEN Tg mice in vivo. (A+C) Representative set of FACS plots indicating CD25^{hi}CD127^{lo}Tregs in peripheral blood **(A)** or spleen **(C)** of humanized NSG mice treated with

a vehicle control (left plots) or a NFAT5 inhibitor (right plots) at 3mg/kg i.p. every day over 4 days. **(B)** Frequencies of $CD25^{hi}CD127^{lo}$Tregs as in **(A)** (n=4 mice per group). **(D)** Frequencies of $CD25^{hi}CD127^{lo}$Tregs as in **(C)** (n=4 mice per group). **(E)** Representative FACS plots indicating $CD25^{+}FoxP3^{+}$Tregs in lymph nodes of PTEN Tg animals after treatment with vehicle control (left plot) or a NFAT5 inhibitor at 3mg/kg i.p. for every day for 7 days (right plot). **(F)** Frequencies of $CD25^{+}FoxP3^{hi}$Tregs as in **(E)** (n=5 mice per group). Data are presented as box and whisker plots with min to max values for data distribution. Student´s t-test. * $p<0.05$, *** $p<0.001$.

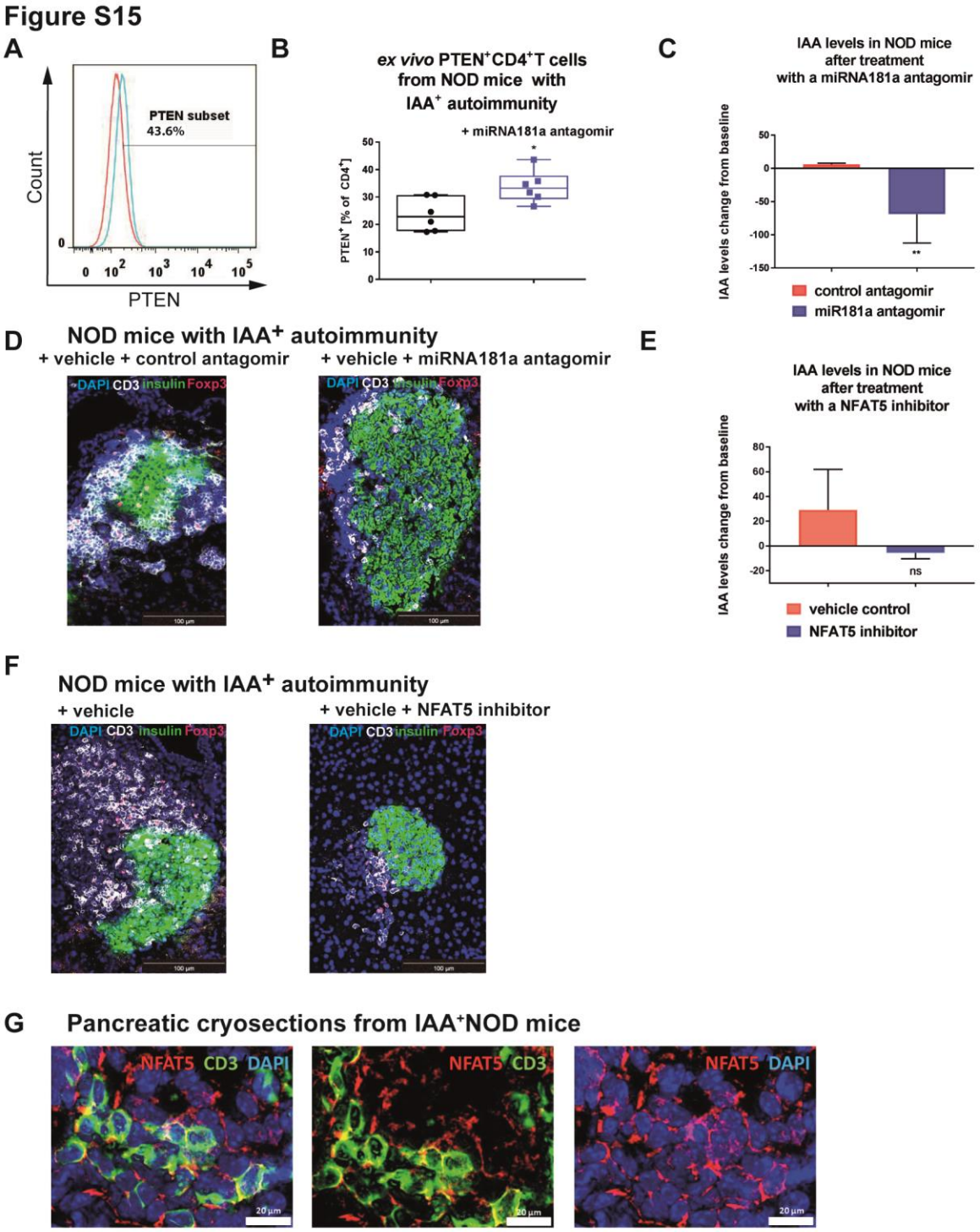

Fig. S15. Reduction of immune activation by blocking miRNA181a or NFAT5 in NOD mice.

(A) Representative histogram of PTEN staining in *ex vivo* $CD4^+$T cells from IAA^+NOD mice treated with a control antagomir (red) or miRNA181a antagomir (blue) at 10 mg/kg i.p. every other day for 14 days. **(B)** Summary graph of $PTEN^+$T cells as in **(A)** (n=6 mice per group). **(C)** IAA levels in serum of NOD mice after treatment with either a control antagomir or a miR181a antagomir as in **(A)**. Data are presented as change from baseline (n=3 mice for control antagomir, n=5 mice for miRNA181a antagomir). **(D)** Immunofluorescent staining for insulin (green), CD3 (white) and FoxP3 (red) in pancreas cryosections of IAA^+NOD mice treated as in **(A) (**n=3 mice per group for control antagomir; n=5 mice for miRNA181a antagomir, 3 sections/mouse, scale bar: 100 µm). **(E)** IAA levels in serum of NOD mice treated with a NFAT5 inhibitor at 3 mg/kg i.p. every day for 14 days. Data are presented as change from baseline (n=5 mice for vehicle control, n=3 mice for NFAT5 inhibitor). **(F)** Immunofluorescent staining for insulin (green), CD3 (white) and FoxP3 (red) in pancreas cryosections of IAA^+NOD mice treated as in **(E)** (n=5 mice for vehicle control, n=3 mice for NFAT5 inhibitor, 3 sections/mouse, scale bar: 100 µm). **(G)** Colocalization of NFAT5 and CD3 or NFAT5 and DAPI in pancreatic cryosections of IAA^+NOD mice (n=5 mice for vehicle control, n=3 mice for NFAT5 inhibitor, 3 sections/mouse, scale bar: 20 µm). Data are presented as box and whisker plots with min to max values for data distribution **(B)** or as mean ± s.e.m. **(C+E)**. Student´s test. * $p<0.05$, ** $p<0.01$, ns $p>0.05$.